Palaeogeography, Palaeoclimatology, Palaeoecology 396 (2014) 17–25

Contents lists available at ScienceDirect

Palaeogeography, Palaeoclimatology, Palaeoecology

journal homepage: www.elsevier.com/locate/palaeo

Impact of monsoons, temperature, and CO_2 on the rainfall and ecosystems of Mt. Kenya during the Common Era

Bronwen Konecky [a,*], James Russell [a], Yongsong Huang [a], Mathias Vuille [b], Lily Cohen [a], F. Alayne Street-Perrott [c]

[a] Department of Geological Sciences, Brown University, Box 1846, Providence, RI 02912, USA
[b] Department of Atmospheric and Environmental Sciences, University at Albany, SUNY, 1400 Washington Ave., Albany, NY 12222, USA
[c] Department of Geography, College of Science, Swansea University, Singleton Park, Swansea SA2 8PP, United Kingdom

ARTICLE INFO

Article history:
Received 23 August 2013
Received in revised form 20 December 2013
Accepted 24 December 2013
Available online 7 January 2014

Keywords:
East Africa
Paleoclimate
Common Era
Hydrogen isotopes
Carbon isotopes
Leaf waxes

ABSTRACT

Glacial and early Holocene-age sediments from lakes on Mt. Kenya have documented strong responses of montane hydrology, ecosystems, and carbon cycling to past changes in temperature and atmospheric CO_2 concentrations. However, little is known about climate and ecosystem variations on Mt. Kenya during the Common Era (the past ~2000 years), despite mounting evidence for significant climate changes in the East African lowlands during the past millennium and recent observations of alpine glacier retreat in the East African highlands. We present a new, high-resolution record of the hydrogen and carbon isotopic composition of terrestrial plant wax compounds (δD_{wax}, $\delta^{13}C_{wax}$) preserved in the sediments of Sacred Lake from 200C.E. to the end of the 20th century. We find that Mt. Kenya's climate was highly variable during the past 1800 years. Droughts at Sacred Lake around ~200C.E., 700C.E., and 1100C.E. align with similar droughts in central Kenya and Uganda/Congo, indicating that failures of both the Indian and Atlantic monsoons caused widespread drought throughout equatorial East Africa during the early Common Era. In contrast, dry and wet periods at Sacred Lake during the past 500 years show meridional and zonal contrasts with other sites in East Africa, suggesting strong spatial heterogeneity, possibly due to independent waxing and waning of the Atlantic and Indian monsoons. Pronounced drying after ~1870C.E. suggests that the current dry phase observed at Sacred Lake may have begun prior to the 20th century, around the time when the retreat of Mt. Kenya's glaciers was first observed by European explorers. Mt. Kenya's vegetation responded strongly to these recent climate changes, highlighting the particular sensitivity of tropical montane climate and ecosystems to regional and global climate patterns, and underscoring the critical need to understand potential impacts of future climate change scenarios on this highly sensitive region.

1. Introduction

1.1. The Common Era in East Africa

The climate of tropical East Africa has fluctuated dramatically over the Common Era (the past ~2000 years; C.E.), with severe, multi-century droughts and pluvials that likely impacted human populations living in the region (Verschuren et al., 2000; Russell and Johnson, 2005). A growing number of paleoclimate reconstructions from tropical East Africa have revealed that the sign, magnitude, and timing of these hydroclimatic anomalies varied widely, most notably during the past ~700 years when available records are most abundant (Russell and Johnson, 2007; Tierney et al., 2013). These spatiotemporal gradients attest to the underlying climatic complexity of the region. East African rainfall is produced by two monsoon systems originating in the tropical Atlantic and Indian Oceans (Nicholson, 1996). Strong interannual rainfall variability arises from interactions between these monsoons and the El Niño/Southern Oscillation (ENSO), the Indian Ocean Dipole (IOD), variations in local and remote sea surface temperature (SST), and the position and strength of convergence along the Intertropical Convergence Zone (ITCZ) (Nicholson, 1996, 1997; Goddard and Graham, 1999; Giannini et al., 2008). Long-term variations in East African climate during the Common Era were likely influenced by low-frequency dynamics of these processes and their effects on the Atlantic and Indian Ocean monsoons, possibly driven by forcing from CO_2, solar output, and resulting global temperatures (Verschuren et al., 2000; Alin and Cohen, 2003; Street-Perrott et al., 2004; Tierney et al., 2010). However, the impact of these coupled processes on tropical East African climate variability remains very poorly understood, as high-resolution paleoclimate records extending beyond ~1000C.E. are scarce. Moreover, tropical montane rainfall and ecosystems have not been extensively studied during the

* Corresponding author. Tel.: +1 404 894 3893.
E-mail address: bkonecky@eas.gatech.edu (B. Konecky).

0031-0182/$ – see front matter © 2014 Elsevier B.V. All rights reserved.
http://dx.doi.org/10.1016/j.palaeo.2013.12.037

Common Era, despite strong sensitivity to climate forcings on longer timescales (Bonnefille and Mohammed, 1994; Street-Perrott et al., 1997; Thompson et al., 2002) and marked 20th century glacial retreat (Hastenrath, 1984, 2001; Moelg et al., 2009). This lack of records from higher elevations in East Africa makes it difficult to contextualize recent changes in montane environments or to assess potential connections between low- and high-elevation climate variations.

We reconstruct paleohydrologic variations during the Common Era using sediments from Sacred Lake, Kenya (0°03′N, 37°32′E; 2350 m asl; Fig. 1). Sacred Lake is a small (~1 km diameter) crater lake situated in undisturbed humid tropical montane forest on the northeastern slope of Mt. Kenya, eastern equatorial East Africa (Street-Perrott et al., 2004). The lake had a maximum depth of approximately 5 m in 1989, though its level is now so low that it is seasonally dry (H. Eggermont, pers. comm.). The lake's mid-slope location on Mt. Kenya lends it a relatively high amount of annual rainfall (>1500 mm/year; Thompson, 1966), primarily falling during two rainy seasons, March–May (MAM) and October–December (OND), with intervening drier seasons during January–February (JF) and June–September (JJAS) (Fig. 1c).

This bimodal rainfall pattern, common to most of equatorial East Africa, results from the twice-annual passage of the Intertropical Convergence Zone (ITCZ) and its associated tropical rain belt over the region (Nicholson, 1996; Verschuren et al., 2000; Russell and Johnson, 2005). During both rainy seasons, Mt. Kenya is located beneath this zone of convergence. The primary moisture source is from the southeast (Fig. 1c) (Draxler, 1999; Russell and Johnson, 2007; Tierney et al., 2013), highlighting the importance of convergence and topographic uplift to rainfall on Mt. Kenya, particularly in the band of maximum rainfall on its southern and eastern flanks (Hastenrath, 1984; Nicholson, 1996). On a regional scale, the MAM and OND rainy seasons are largely uncorrelated; although most of equatorial East Africa receives more rainfall on average during the MAM "long rains," the OND "short rains" season is responsible for the majority of interannual variability (Nicholson, 1996, 1997; Goddard and Graham, 1999; Giannini et al., 2008). In contrast, Sacred Lake receives a similar amount of precipitation during both OND and MAM (Fig. 1c), and its slope exposure makes it highly sensitive to the intensity of northeasterly winds during the dry monsoon season (Jan–Feb) (Hastenrath, 1984; Street-Perrott et al., 2004). That Sacred Lake receives a similar or greater amount of rainfall during OND than MAM provides an important contrast to other records from the region that are dominated by the MAM "long rains" season (Fig. 1).

Sacred Lake's slope position also makes it a sensitive recorder of changes in montane vegetation (e.g. Street-Perrott et al., 2004), providing a unique opportunity to investigate changes in Mt. Kenya's montane ecosystems during the Common Era. The climate and vegetation of Mt. Kenya are altitudinally graded into three general belts: montane forest (from ~1500 to ~3500 m asl), ericaceous tall shrubland (~3500–4000 m asl), and afroalpine shrub grassland (4000–4500 m asl) (Coetzee, 1967). In the past 26,000 years, the catchment of Sacred Lake has been occupied by all three of Mt. Kenya's main vegetation belts,

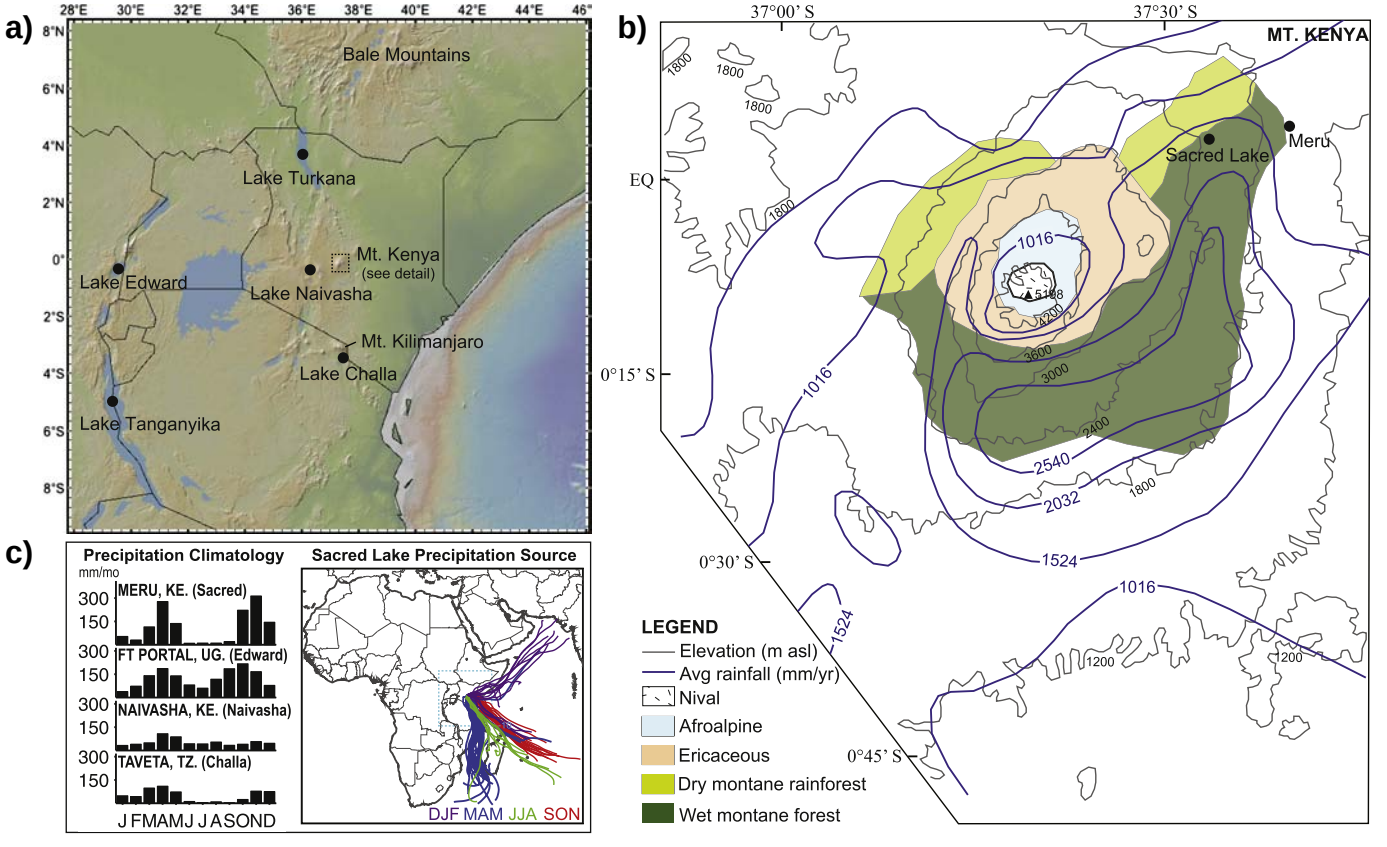

Fig. 1. a) Map of equatorial East Africa and of sites discussed in the text (http://www.geomapapp.org). b) Detailed map of Mt. Kenya depicting rainfall and vegetation zones and location of Sacred Lake. Shaded regions correspond to vegetation zones, and bold/blue contours depict average annual rainfall. Topographic map and vegetation zones are adapted from Huang et al. (1999) and Street-Perrott et al. (2004), and average rainfall is adapted from Thompson (1966). c) Left: Precipitation climatology from the Global Historical Climatology Network for meteorological stations adjacent to Sacred Lake (Meru, Kenya), Lake Edward (Fort Portal, Uganda), Lake Naivasha (Naivasha, Kenya), and Lake Challa (Taveta, Tanzania). Right: Back-trajectories of rain-bearing air masses arriving at Sacred Lake from July 2003–June 2004 (a "normal" year with little to no ENSO or IOD activity). Trajectories were modeled using the Hybrid Single Particle Lagrangian Integrated Trajectory Model (HYSPLIT; NOAA/ARL, Draxler, 1999) with the NCEP/NCAR Reanalysis 2.5 degree gridded dataset. 7-day trajectories were calculated every 12 h for one full year. Only trajectories that produced >0.5 mm/h of precipitation within 12 h of reaching the study site are shown. (For interpretation of the references to color in this figure, the reader is referred to the web version of this article.)

and by four different types of montane forest. During the late Holocene, however, the landscape has been occupied solely by humid montane forest (Coetzee, 1964, 1967), as it is today (Fig. 1b). Despite the relative stability of the vegetation belts compared to glacial/interglacial fluctuations, variations in highland vegetation from elsewhere in East Africa reveal that the highlands are highly sensitive to centennial-scale climate fluctuations (Bonnefille and Mohammed, 1994), highlighting the need to investigate recent ecological changes on Mt. Kenya within the context of the Common Era.

1.2. Using sedimentary leaf waxes to track changes in East African precipitation and vegetation

We use the δD of terrestrial leaf wax compounds (δD_{wax}) preserved in the sediments of Sacred Lake to reconstruct variations in the δD of precipitation (δD_{precip}) during the past 1800 years. Stable O and H isotopes in precipitation are useful tools for tracking past variations in tropical rainfall and atmospheric circulation, owing to their strong relationships with rainfall amount, transport trajectory, and convective intensity (Dansgaard, 1964; LeGrande and Schmidt, 2009). In East Africa, stable isotopes in modern precipitation have been shown to reflect large-scale atmospheric circulation processes (Vuille et al., 2005), and the $\delta^{18}O$ of precipitation (and by inference, the δD of precipitation) on Mt. Kenya has been shown to be a good indicator of moisture balance (Barker et al., 2001). Leaf wax δD reflects δD_{precip}, after a series of offsets due to soil water evaporation, fractionation of leaf water relative to xylem water, and biosynthesis (Sachse et al., 2012). This technique has been successfully employed to reconstruct late Quaternary changes in East African monsoon intensity, rainfall amount, and other atmospheric circulation processes (Berke et al., 2012a).

The carbon isotopic composition of leaf waxes ($\delta^{13}C_{wax}$) can provide important information about changes in vegetation through time (Collister et al., 1994). Changes in the $\delta^{13}C$ of bulk or compound-specific plant material can arise from temperature, altitude, and water stress, as well as phylogeny and physiology (O'Leary, 1981; Diefendorf et al., 2010). Bulk plant material from C_3 plants surveyed on Mt. Kenya exhibit a ~10‰ range in their $\delta^{13}C$ values, with a much smaller range (<3‰) found within the C_4 group, consistent with global studies (O'Leary, 1981; Ficken et al., 2000; Wooller et al., 2001). Variations between C_3/C_4 plants, however, can result in $\delta^{13}C$ variations from 11–25‰ (Ficken et al., 2000; Wooller et al., 2001). On glacial/interglacial timescales, the $\delta^{13}C$ of terrestrial plant wax compounds in sediments of Sacred Lake has been shown to primarily reflect the interplay between plants using the C_3 vs. the C_4 photosynthetic pathway (Huang et al., 1999). Variations in the relative abundance of C_3/C_4 plants from the Last Glacial Maximum (LGM) to present on Mt. Kenya mainly reflects climate-driven changes in the altitudinal distribution of C_3-dominated tropical montane forest and ericaceous/afroalpine zones containing more C_4 vegetation (Huang et al., 1999; Wooller et al., 2001). Large $\delta^{13}C_{wax}$ variations are associated with these changes, e.g. up to a 17‰ glacial-early Holocene difference in $\delta^{13}C$ of the C_{28} *n*-acid. Glacial $\delta^{13}C_{C28}$ values as high as −17.7‰ reflected an expansion of C_4 grasslands due to low atmospheric CO_2 conditions that favor C_4 plants (Collatz et al., 1998). Pronounced aridity may have further supported these ecosystems during the glacial period, but it has been shown that atmospheric CO_2 played the biggest role in C_3/C_4 variations on Mt. Kenya, with a deglacial rise in C_3 plants coinciding with increasing atmospheric CO_2 recorded in Antarctic ice cores (Street-Perrott et al., 1997).

Major ecological changes have the potential to impact δD_{wax} through differences in the apparent, or net, fractionation between wax compounds and precipitation ($\varepsilon_{wax\text{-}P}$) among different plant groups. Certain life forms (e.g. trees vs. shrubs) or classes (e.g. monocotyledonous vs. dicotyledonous) tend to exhibit a stronger apparent D/H fractionation (Sachse et al., 2012). Where possible, we calculate the potential influence of changing vegetation and include these corrections in our analysis. However, Sacred Lake is currently surrounded by undisturbed tropical montane forest, and has been occupied by tropical montane forest types for at least the past 3000 years (Coetzee, 1967). Sacred Lake has been noted for its diverse community of aquatic vegetation, including C_3 emergent macrophytes and C_4 marginal swamp grasses and sedges (Huang et al., 1999; Ficken et al., 2000), which could potentially be a source for long-chain *n*-alkanoic acids in its sediments. However, previous work has demonstrated that waxes from the dense terrestrial vegetation surrounding Sacred Lake overwhelm any potential aquatic source (Huang et al., 1999). Long-chain ($>C_{25}$) *n*-alkyl lipids (including *n*-alkanoic acids) in Sacred Lake's sediments come primarily from terrestrial plants, based on downcore covariation of $\delta^{13}C$ from multiple types of *n*-alkyl lipids characteristic of terrestrial plants and a low abundance of short-chain fatty acids characteristic of algae (Huang et al., 1999). We calculate the Average Chain Length (ACL) of our samples and compare with our δD_{wax} values to provide an additional assessment of changes in vegetation type.

2. Methods

Sediment core SL1 was recovered from 2.5 m water depth in 1989 (Olago et al., 2000), then archived in cold storage (4 °C) at Swansea University, UK. 97 samples for plant wax isotopic analysis were subsampled from the upper 2.5 m of SL1 in 2010. To purify wax compounds, sediments were freeze-dried, homogenized, and extracted using a Dionex 350 Accelerated Solvent Extractor. Fatty acids were then purified following the methods of Konecky et al. (2011). The δD and $\delta^{13}C$ of the C_{28} *n*-alkanoic acid, the most abundant homologue in all samples, were measured using gas chromatography isotope ratio mass spectrometry at Brown University. Hereafter, we refer to the δD and the $\delta^{13}C$ of C_{28} *n*-alkanoic acid as δD_{wax} and $\delta^{13}C_{wax}$, respectively. δD_{wax} was measured on 97 samples and $\delta^{13}C_{wax}$ was measured on a randomly selected subset of 28 samples. Samples were run at least in duplicate for both δD and $\delta^{13}C$, with precision of between 0.01–3.00‰ for δD_{wax} and between 0.01–0.52‰ for $\delta^{13}C_{wax}$. After every six injections, a synthetic standard containing C_{16}–C_{28} fatty acid methyl esters of known δD and $\delta^{13}C$ was injected to monitor machine performance and to calculate standard error. Because precision is slightly higher on synthetic standards than on real samples, we also ran a subset of samples in triplicate to produce a more robust error estimate. The pooled δD_{wax} standard deviation from 7 triplicate samples was 1.65‰, and the pooled $\delta^{13}C_{wax}$ standard deviation from 5 triplicate samples was 0.17‰. All δD_{wax} and $\delta^{13}C_{wax}$ values are reported relative to Vienna Standard Mean Ocean Water (VSMOW) and Vienna Pee Dee Belemnite (VPDB), respectively, and have been corrected for the methyl group added during derivatization.

An age model for the full length of core SL1 (16.34 m; >40,000 years of sediment) was constructed using a mixed effect regression model (Heegaard et al., 2005) based on 29 radiocarbon dates on bulk organic matter (Loomis et al., 2012). Several substantial changes in sedimentation rate occur in deeper sections of the core, the uppermost of which is around 365 cm depth. Because ^{14}C ages in the upper 3 m of core suggest much more linear sedimentation rates, and our samples extend only to 2.5 m, we constructed a new age model for the upper 3 m of core using the 8 uppermost radiocarbon dates. We assume a core-top age of 1989C.E., the year of core collection. Our mixed-effect regression age model is presented in Fig. 2.

3. Results and discussion

Leaf wax δD varies nearly 40‰, between −100.6‰ and −138.3‰ over the past 1800 years (Fig. 3), with prominent centennial-scale variations on the order of 10‰. These variations are superimposed upon a longer-term fluctuation in δD_{wax}, with the most D-enriched waxes occurring at 200C.E. and after 1960C.E., and the most D-depleted waxes in between, with a minimum δD_{wax} value at ~1400C.E. Changes in C_3/C_4 vegetation (see below) could change the magnitudes of some of

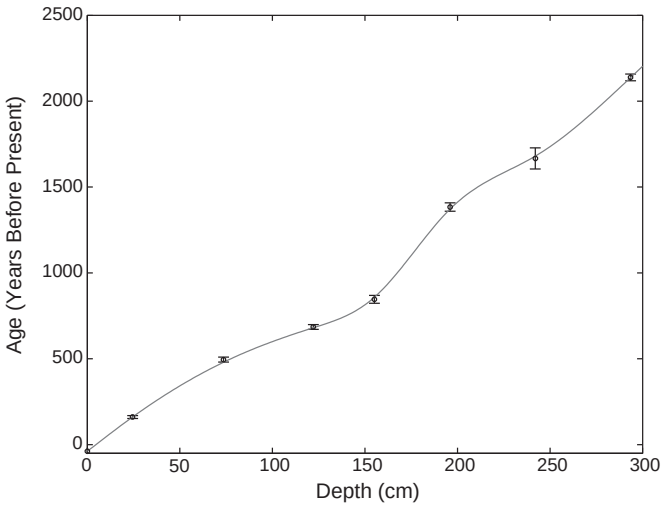

Fig. 2. Age model for sediment core SL1 (see text for details).

these fluctuations in δD_{wax}, as the apparent fractionation between precipitation and leaf wax compounds ($\varepsilon_{wax\text{-}P}$) for C_3 vs. C_4 plants can differ by ~20‰ (Sachse et al., 2012). Accounting for these effects can change the absolute value of reconstructed δD_{precip} by up to 11‰, but variations in $\delta^{13}C_{wax}$ are too small to alter the overall structure of the record (Fig. S1). Due to this and to the continuing uncertainty regarding the exact amplitudes of these corrections for *n*-alkanoic acids derived from African vegetation, we discuss uncorrected δD_{wax} values below. Both corrected and uncorrected δD_{precip} are presented in Fig. S1. Additionally, the Average Chain Length (ACL) of fatty acids, which is an indication of changes in vegetation type, shows no strong relationship with δD_{wax} in our record ($r^2 = 0.03$, $p > 0.05$). Therefore, changes in terrestrial or aquatic vegetation are not likely to have driven the δD_{wax} signal at Sacred Lake over the past 1800 years.

3.1. Variations in Indian Ocean monsoon rainfall in tropical East Africa during the Common Era

The sediments of Sacred Lake provide an important contrast to other equatorial paleoclimate reconstructions from East Africa (Verschuren et al., 2000; Russell and Johnson, 2007; Tierney et al., 2011, 2013). Unlike equatorial lakes from Uganda and central Kenya (west of Mt. Kenya), Sacred Lake currently receives no Atlantic-derived precipitation, and its elevation, northeastern slope exposure, and rainfall seasonality make it particularly susceptible to changes in the Indian Ocean monsoons. In contrast, equatorial lakes in central Kenya (e.g. Lake Naivasha) and the western Rift Valley (e.g. Lake Edward, Uganda/Congo) receive a mixture of Indian- and Atlantic-derived moisture, and hence are sensitive to both monsoons (Nicholson, 1996). East/west spatial gradients in these sites' rainfall histories therefore provide insight into the two competing monsoon systems that provide moisture for East Africa, and their interactions with regional and global climate changes during the Common Era. North/south contrasts between Sacred Lake and Lake Challa, located at a similar longitude but at 3°S in the southeastern lowlands of Mt. Kilimanjaro, provide an important perspective on the seasonal character of Indian Ocean rainfall variations during the Common Era (Tierney et al., 2011). Lake Challa receives primarily Indian Ocean-derived precipitation, but with a higher proportion falling during MAM, contrasting with Sacred Lake's nearly equal rainy seasons and relatively high contribution of OND rainfall (Fig. 1).

The Sacred Lake δD_{wax} record is marked by centennial-scale variability. Three major D-enrichments occurred during the early Common Era: at 200C.E., from 620–750C.E, and from 1050–1150C.E. These three D-enrichments, each on the order of approximately 10‰, are consistent in timing with other East African lake records indicating severe and widespread drought across much of tropical East Africa from 0–200C.E. and 1000–1200C.E., and a pronounced but more spatially limited drought from 540–890C.E. (Fig. 3) (Verschuren, 2001; Alin and Cohen, 2003; Russell and Johnson, 2005). Because Sacred Lake's precipitation is purely derived from Indian Ocean sources, D-enrichments during these intervals indicate that these regional-scale droughts were driven at least in part by a weakening of the Indian Ocean monsoon. Weakening of the Atlantic monsoon also played its own role in these droughts, however, particularly from 1000–1200C.E., when sites that are sensitive to both the Indian and Atlantic monsoons experienced severely dry conditions (Fig. 3). This dry interval recorded at Lakes Naivasha (Kenya), Edward (Uganda/Congo), and Tanganyika (Tanzania/DRC) corresponds to a shorter (~100 year) D-enrichment in waxes at Sacred Lake (Verschuren, 2001; Alin and Cohen, 2003; Russell and Johnson, 2005). This, together with the evidence for dry conditions at this time from West Africa, suggests that severe drought in Uganda/Congo and central Kenya from 1000–1200C.E. was mainly driven by reduced penetration of the Atlantic monsoon into equatorial East Africa (Shanahan et al., 2009), rather than a failure of the Indian Ocean monsoon. A shorter-lived or less pronounced weakening of the Indian Ocean monsoon may have exacerbated drought conditions in the region from 1050–1150C.E.

Following the 1050–1150C.E. drought, Sacred Lake δD_{wax} becomes more D-depleted, with low variability, until approximately 1400C.E, indicating relatively wet and stable hydrological conditions. Lakes Edward and Naivasha also show wetter overall conditions during this time, but punctuated by several decadal-scale droughts (Fig. 3). This spatial pattern may indicate a general strengthening of both monsoon systems, with decadal-scale variability in the Atlantic monsoon that caused rainfall variations in Uganda and western Kenya. The Mt. Kilimanjaro ice core $\delta^{18}O$ record indicates wet and/or cool conditions during this time, although Lake Challa δD_{wax} indicates weaker monsoon circulation (Thompson et al., 2002; Tierney et al., 2011), suggesting that Indian Ocean-derived moisture may have been more variable in the southern equatorial latitudes. Wet conditions at Sacred Lake, Lake Edward, and Lake Naviasha from 850–1000C.E. and 1200–1450C.E. may have been enhanced by a more northern position of the ITCZ (Haug et al., 2001). A northward-displaced ITCZ would have led the tropical rain belt in East Africa to spend more time in the northern tropics, tempering the effects of intensified monsoon circulation on Lake Challa, which experienced more moderate conditions (Fig. 3).

The strong similarities in equatorial East African climate variations from 200–1400C.E. stand in contrast to the spatiotemporal heterogeneity that characterizes the region's hydrology after 1400C.E. The Northern Hemisphere "Little Ice Age" (LIA; 1450–1850C.E.) was particularly temporally and spatially complex within East Africa (Fig. 3). Hydrological anomalies are evident at many locations, but the sign of these anomalies as well as their temporal evolution vary dramatically from site to site, both in the early LIA (1450–1700C.E.) and the late LIA (1700–1850C.E.) (Verschuren et al., 2000; Russell and Johnson, 2007; Tierney et al., 2011, 2013).

At the start of the early LIA (~1450C.E.), Sacred Lake, Lake Edward, and Lake Naivasha all experienced rapid drying, with pronounced aridity between ~1520–1560C.E. (Fig. 3). Sacred Lake and Lake Edward remained dry until the late LIA, ~1700C.E., with decadal-scale droughts at Sacred Lake centered at 1610 and 1680C.E. that are possibly aligned with decadal-scale features at Lake Edward. Concurrently, Lakes Naivasha and Challa experienced increasingly wet conditions beginning ~1600C.E. during the early LIA. This regional heterogeneity is difficult to reconcile from variations in the Atlantic and/or the Indian monsoons. The onset of dry conditions at the start of the early LIA and highly variable Sacred Lake δD_{wax} thereafter should indicate that the Indian Ocean monsoon caused strong fluctuations in East African moisture balance; however, these fluctuations are not evident at Lake Challa, which also receives primarily Indian Ocean derived precipitation. Instead, Sacred

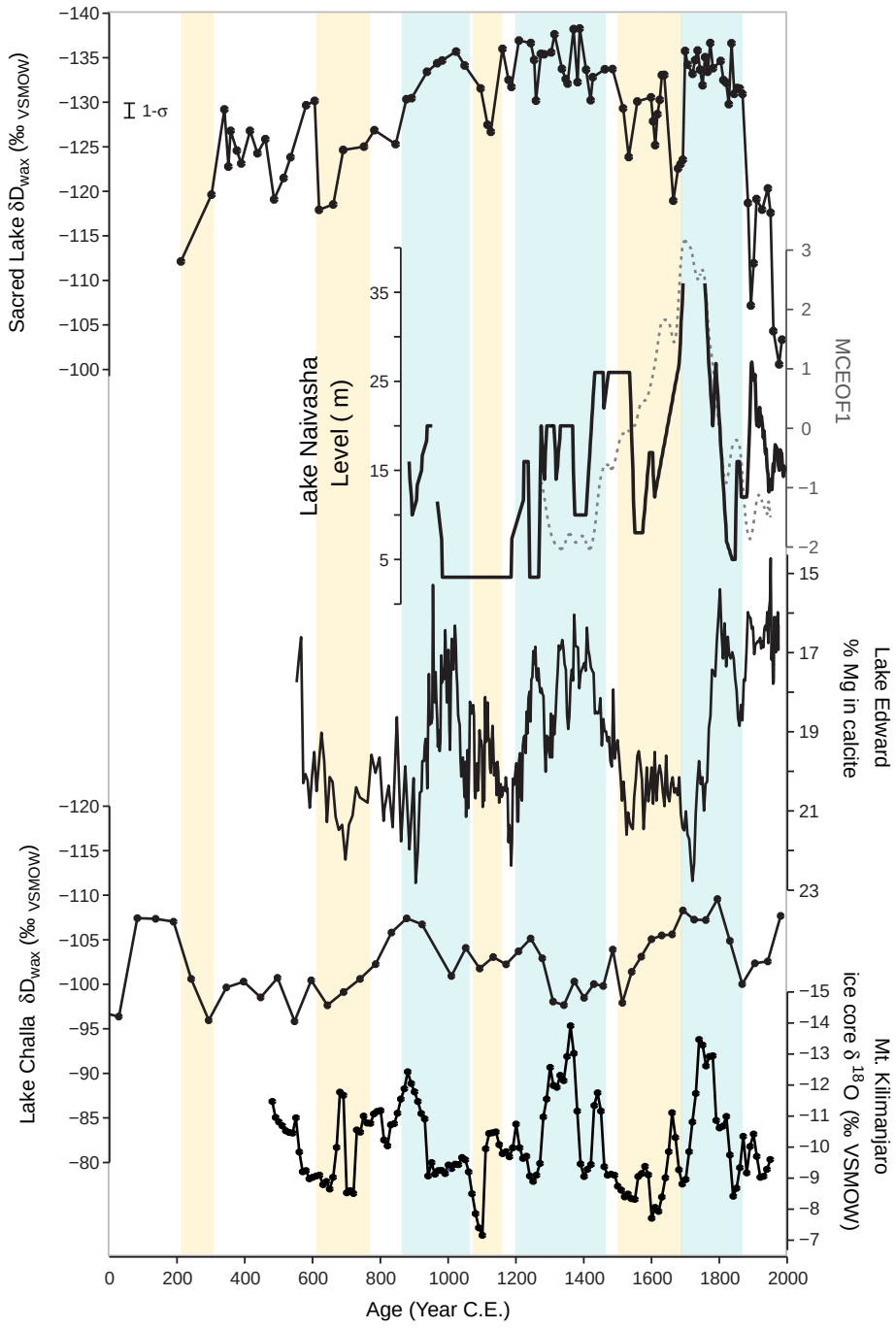

Fig. 3. Sacred Lake δD_{wax} and paleoclimate reconstructions from Lake Naivasha, Kenya (Verschuren et al., 2000); the first Empirical Orthogonal Function (MCEOF1) from a 700-year synthesis of multiple hydroclimate records across East Africa (Anchukaitis and Tierney, 2012; Tierney et al., 2013); moisture balance of Lake Edward, Uganda/Congo, derived from the Mg/Ca ratio in authigenic calcite (Russell and Johnson, 2007; 2005); δD_{wax} from Lake Challa, Tanzania (Tierney et al., 2011); and $\delta^{18}O$ of ice, an integrated atmospheric tracer, preserved at the summit of Mt. Kilimanjaro, Tanzania (Thompson et al., 2002). Orange (blue) shading represents centennial-scale D-enriched (D-depleted) intervals in δD_{wax} discussed in the text. (For interpretation of the references to color in this figure, the reader is referred to the web version of this article.)

Lake δD_{wax} shares more similarities with hydroclimatic reconstructions from Lake Edward, in western Uganda, while Lake Naivasha (between Lake Edward and Sacred Lake) and Lake Challa (south of Sacred Lake) exhibit very different behavior. A southward shift of the ITCZ during the Little Ice Age (Haug et al., 2001) may have mitigated the effects of the weaker Indian Ocean monsoon on Lake Challa during the early LIA, while causing more severe dry conditions at equatorial sites (Fig. 3). Alternatively, early LIA monsoon variations could have been highly seasonal in character, with reduced precipitation during the OND season associated with the Indian Winter Monsoon. Sacred Lake and Lake Edward receive disproportionately more of their precipitation during OND than MAM, while Challa and Naivasha, receive more MAM precipitation (Fig. 1c). A weaker northeasterly Indian Winter Monsoon could have enhanced these effects at high elevations, as both Sacred Lake and the summit of Mt. Kilimanjaro record isotopically enriched precipitation during the early LIA, concurrent with dry conditions in western East Africa (Fig. 3).

In the late LIA (1700–1850C.E.), precipitation anomalies in tropical East African proxy records are more coherent in timing and magnitude (Fig. 3). Sacred Lake δD_{wax} transitions abruptly into pluvial conditions

at 1700C.E., with a ~10‰ D-depletion relative to the preceding dry conditions. The late-LIA pluvial at Sacred Lake is contemporary to a primary mode of variability during the past 700 years found in a recent multi-site analysis of tropical East African proxy records, where a pluvial ca. 1700C.E. (Tierney et al., 2013) was found to be robust even when age model uncertainties were taken into account (Anchukaitis and Tierney, 2012). The onset of pluvial conditions is markedly similar, though more abrupt, to the onset of pluvial conditions observed at Lake Naivasha, which overflowed from 1670–1770C.E. (Verschuren et al., 2000), and to severe drought conditions observed contemporaneously at Lake Edward (Fig. 3) and Lake Tanganyika, supporting previous findings that easternmost East Africa generally experienced pluvial conditions during the late LIA while western and southern East Africa experienced drought (Russell and Johnson, 2007; Tierney et al., 2013).

Previous studies of LIA climate in East Africa suggested that the east/west spatial gradient in rainfall in the equatorial tropics may have been caused by either more El Niño-like conditions combined with a southward-displaced ITCZ (Russell and Johnson, 2007) or by low-frequency variations in the Indian Ocean Walker circulation (Tierney et al., 2013). Either of these mechanisms could be supported by reconstructed SST in the Indo-Pacific Warm Pool, which reached peak cool conditions during the late LIA, corresponding to pluvial conditions in East Africa (Oppo et al., 2009; Tierney et al., 2013). On modern, interannual timescales, El Niño events and IOD positive events lead to wetter conditions in equatorial Africa and drier conditions in southern Africa, partly due to the intensification of the OND rainy season in easternmost equatorial East Africa, and partly due to the modification of westerly moisture transport across the Congo Basin and into western East Africa (Nicholson and Kim, 1997; Saji et al., 1999; Ummenhofer et al., 2009). However, drying of western equatorial East Africa during the OND season is not a characteristic feature of these events in either observations or in model simulations (Nicholson and Kim, 1997; Ummenhofer et al., 2009), even in cases when surface moisture flux divergence anomalies occur (Goddard and Graham, 1999; Ummenhofer et al., 2009). In fact, both western Uganda and Lake Tanganyika generally experience wetter conditions during IOD+ and El Niño events (Bergonzini et al., 2004; Ummenhofer et al., 2009), just as eastern East Africa does. Hence, while an El Niño-like mode or enhanced Indian Walker circulation could have contributed to pluvial conditions along the East African coast during the late LIA, these mechanisms are not sufficient to explain the East–west gradient in LIA climate over East Africa.

Both the early-LIA heterogeneity across East Africa and the late-LIA drought conditions in western equatorial East Africa suggest complex interactions between the Indian and Atlantic monsoons, the ITCZ, and the transport of westerly moisture across the continent. Although failure of the West African monsoon was restricted mostly to the early LIA (Shanahan et al., 2009), the ITCZ was in a southerly position during most of the LIA, with its southernmost position from ~1700–1800 (Haug et al., 2001). This resulted in a southward displaced rain belt in East Africa (Brown and Johnson, 2005) that may have dried the continental interior (Russell and Johnson, 2007). A southward-displaced ITCZ could also explain some of the early-LIA similarities between Lake Edward and Sacred Lake (Fig. 3). Since both of these sites are highly influenced by OND rainfall, it is also possible that early LIA droughts were particular to the OND season, with more limited ramifications for sites that receive more MAM rainfall. From these findings, it is clear that the "LIA" in East Africa was in fact composed of a series of climatic events, with the most pronounced variability occurring after 1700C.E. when peak wet/dry conditions characterized the eastern/western sites, respectively.

In addition to pronounced centennial-scale variability, δD_{wax} at Sacred Lake exhibits a gradual trend over the past 1800 years. δD_{wax} is over 15‰ more D-depleted from ~1000C.E.–1400C.E. and ~1700–1850C.E. than at the start of our record (200C.E.) and after 1850C.E. Although few equatorial East African records contain data prior to 600C.E. for comparison, no long-term trend over the Common Era is evident in other paleo-hydrological reconstructions (Fig. 3). The progressive δD_{wax} depletion and subsequent enrichment may reflect increased and decreased fractionation taking place upstream of Mt. Kenya, for example via the strength of convection and rainout over the Indian Ocean. However, decreased rainout over the Indian Ocean would also result in isotopically heavier precipitation in the Indian and Asian Monsoon region, but D-enrichment at Sacred Lake between ~200–1000C.E. and after 1850C.E. corresponds generally to strengthened, not weakened, Asian Monsoon (Zhang et al., 2008).

The long-term trend in δD_{wax} could represent a gradual weakening and strengthening of equatorial westerlies in the Indian Ocean, bringing more followed by less precipitation to East Africa, as is the case on centennial timescales (Hastenrath, 2001). However, the magnitude of this long-term trend compared with relatively small (if any) long-term trends in other records suggests that H-isotopic fractionation may be locally enhanced at Sacred Lake. This could arise due to the site's strong sensitivity to OND rainfall or to feedbacks over wet montane forests enhancing cloudiness and convection (Hastenrath, 1984; Hemp, 2006). Alternatively, this enhancement could be an indirect, local response to changes in air temperature in East Africa during the Common Era. Air temperatures at Sacred Lake were generally ~1 °C cooler from 800–1500C.E. (Loomis et al., 2012), when waxes are most D-depleted, and lake surface temperatures in the East African lowlands suggest that the late LIA was 1–2 °C cooler than during the 20th century (Tierney et al., 2010; Powers et al., 2011; Berke et al., 2012b). Temperature variations in this equatorial location are too small to significantly affect δD_{precip} via direct kinetic effects on the D/H fractionation factor at the time of condensation (Dansgaard, 1964; Majoube, 1971) or via evaporation of soil water (Craig and Gordon, 1965; Dagg and Blackie, 1970; Riley et al., 2002), but air temperature is important for the elevation of the zone of maximum rainfall (ZMR) on Mt. Kenya. The ZMR currently sits 150 m higher than Sacred Lake, at a mid-slope elevation of 2500–3000 m asl (Hastenrath, 1984), focused on the southeastern flank where exposure to the southeastern monsoon is most direct (Fig. 1, Thompson, 1966). Assuming no major change in prevailing wind direction, absolute humidity, or temperature lapse rate (Eggermont et al., 2010), a cooling should lead to condensation at lower elevations, bringing the ZMR closer to Sacred Lake. Even small downslope migrations of the ZMR could enhance D-depletion of δD_{precip} at Sacred Lake via the combined effects of increased rainfall amount, increased humidity, and lower evaporative losses (and hence reduced D-enrichment) from increased cloud cover (Bruijnzeel et al., 2011). Additional high-elevation temperature/δD_{precip} reconstructions from Mt. Kenya and other tropical mountains are needed to test this hypothesis, but this mechanism is plausible considering the high sensitivity of tropical mountains to regional and global temperature changes (Bradley et al., 2009) and the importance of low-elevation temperatures to lapse rates and moisture gradients on nearby Mt. Kilimanjaro (Duane et al., 2008).

3.2. Aridification and ecological change on Mt. Kenya since 1870C.E.

In recent years, Sacred Lake levels have dropped to the point at which it is at times desiccated (H. Eggermont, pers. comm.). Our δD_{wax} record reveals an abrupt, nearly 30‰ D-enrichment after 1870C.E., suggesting aridification on Mt. Kenya. This D-enrichment progresses in two stages: a 20‰ D-enrichment between 1870 and 1895C.E., a return to relatively D-depleted waxes between 1925 and 1950C.E., followed by a 15‰ D-enrichment into the present. The amplitude of this D-enrichment may have been enhanced by a suite of processes shown to drive rainfall in arid regions to become isotopically heavier, such as re-evaporation, recycling, and vertical mixing of moisture from the lowlands (Worden et al., 2007; Levin et al., 2009; Kebede and Travi, 2012; Cockerton et al., 2013). These processes were likely reduced during the wetter climate of the late LIA. Changes in C_3/C_4 vegetation (see below) could also influence the amplitude of this D-enrichment, but the ~30‰ amplitude of the

post-LIA D-enrichment is affected by less than 4‰ when considering vegetation changes (Fig. S1), indicating that the signal is robust.

Historical lake levels from much of East Africa, including nearby Lake Naivasha, also suggest wetter conditions in the late 19th/early 20th centuries, followed by drying during the early 20th century (Nicholson, 2001; Verschuren, 2001, 2004). Our chronology prohibits an exact comparison of the timing between these shifts, but the large enrichment in δD_{wax} after 1870 suggests that this drying trend began prior to the 20th century. The strength of low-level equatorial westerlies in the Indian Ocean has been linked to East African lake levels as well as Mt. Kenya's glaciers, with stronger (weaker) winds inhibiting (enhancing) precipitation in East Africa (Hastenrath, 2001). Overall, these westerlies have increased in strength since the 1880's. This important Indian Ocean forcing may explain Sacred Lake's particular sensitivity to these changes, and recent drying may have also been locally enhanced by a recent rise in temperature (via an upward shift in the ZMR and/or increased evaporation of soil water).

To understand the influence of recent climate changes on Mt. Kenya's forest composition, we turn to stable isotopes of carbon preserved in our leaf wax samples. Over the past 1800 years, $\delta^{13}C_{wax}$ ranges from −30.3‰ to −26.5‰ (Fig. 4). These relatively ^{13}C-depleted values fall within the range of $\delta^{13}C_{C28}$ values reported by Huang et al. (1999) for the Holocene (Fig. 4), and indicate that during the past two millennia, the Sacred Lake catchment contained a C_3-dominated mix of vegetation. $\delta^{13}C_{wax}$ is moderately, positively correlated with ACL ($r^2 = 0.3$, $p < 0.05$), suggesting that ^{13}C-enrichments are from increased inputs from C_4 grasses, which tend to have more long-chain waxes than C_3 forest plants (Vogts et al., 2009).

Prior to 1870C.E., variations in $\delta^{13}C_{wax}$ are generally small (<1‰–2.5‰), with no obvious trend (Fig. 4). Although the resolution of our $\delta^{13}C_{wax}$ dataset is too low to assess variations in C_3/C_4 vegetation during individual centennial-scale hydroclimatic events in our δD_{wax} record, it appears that these droughts and pluvials did not substantially affect the distribution of C_3/C_4 vegetation prior to 1870C.E. C_4 grasses are only minor components in the understory of humid tropical or dry montane rainforest on Mt. Kenya (Wooller et al., 2001), but are abundant in the semi-tropical humid forest zone located at lower elevations on northeastern Mt. Kenya, and CAM plants such as *Euphorbia* and other succulents are present further west on the drier northern flank of Mt. Kenya (Coetzee, 1967; Wooller et al., 2001; Street-Perrott et al., 2004). $\delta^{13}C_{wax}$ and δD_{wax} are strongly, inversely correlated ($r^2 = 0.82$), suggesting that wetter conditions accompany more C_4/CAM inputs. C_4 grasses could flourish when the lowlands are wetter during the growing season (Collatz et al., 1998) and the semi-tropical humid forest prospers, or under greater wet season storm intensity, which favors grasses over woody biomass (Good and Caylor, 2011). CAM plants in the water-stressed northern scrublands could also prosper under slightly wetter conditions. However, pre-industrial variations in $\delta^{13}C_{wax}$ are minor, and thus do not suggest major changes in vegetation until the 18th century (Fig. 4).

In the middle of the 18th century, $\delta^{13}C_{wax}$ begins to substantially decline, with a two-step, ~4‰ ^{13}C-depletion occurring between the 1760s and the 1970s (Fig. 4). This suggests that C_4 vegetation was substantially reduced after the mid-18th century relative to the previous 1550 years, when its contribution was already small. δD_{wax} indicates drying during recent centuries, and one might expect C_4 grasses to flourish relative to C_3 trees under a drying climate. However, temperature and CO_2 are much bigger drivers of large changes in the distribution of C_4 grasses than aridity on Mt. Kenya, including around Sacred Lake, as well as nearby Mt. Elgon (Street-Perrott et al., 1997). C_4 plants are more competitive than C_3 plants at low-CO_2 conditions because they contain a CO_2-concentrating mechanism, but they lose this competitive advantage under high CO_2 conditions (Ehleringer et al., 1997). C_3 plants benefit both directly and indirectly under high atmospheric CO_2 conditions, particularly in water-limited, seasonally dry biomes of tropical East African mountains (Jolly and Haxeltine, 1997). Increased CO_2 reduces stomatal conductance and transpiration, and directly modulates the activity of the primary enzyme used in C_3 photosynthesis, thereby increasing photosynthetic efficiency (Sage, 2002; Sage et al., 2008). The photosynthetic efficiency of C_4 plants, however, is not significantly affected by atmospheric CO_2 (Collatz et al., 1998), giving C_3 plants a relative advantage (Ehleringer et al., 1997).

Modern mean annual air temperature in the East African lowlands averages approximately ~22 °C (Loomis et al., 2012), within the range of temperatures where both the C_3 and the C_4 photosynthetic pathways are favored under both 20th century and pre-industrial atmospheric CO_2 concentrations (280 ppm, Etheridge et al., 1996). Sacred Lake, on the other hand, has a mean annual air temperature of 14.9 °C (Loomis et al., 2012). At pre-industrial CO_2 levels this temperature places Sacred Lake at the boundary between C_3- and C_4-favorable CO_2 and temperature conditions (Ehleringer et al., 1997; Collatz et al., 1998). The post-industrial rise in atmospheric CO_2 (Etheridge et al., 1996) would have distinctly favored C_3 plants (Ehleringer et al., 1997), even at lower altitudes on Mt. Kenya where temperatures were slightly warmer.

Indeed, this rapid decrease in $\delta^{13}C_{wax}$ closely coincides with increasing atmospheric CO_2 following the Industrial Revolution (Etheridge et al., 1996). Increased CO_2 relative to O_2 and rising temperatures could have increased the rate of C_3 photosynthesis around the elevation

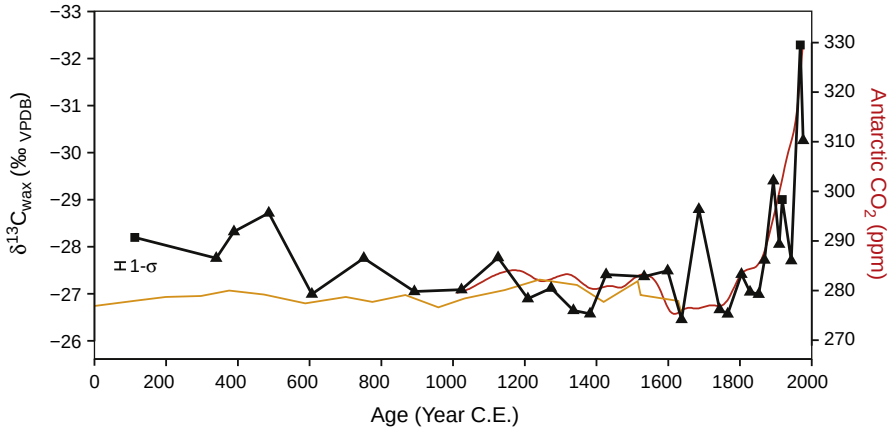

Fig. 4. Sacred Lake $\delta^{13}C_{wax}$ and atmospheric CO_2 reconstructions from Law Dome (red) and EPICA Dome C (orange) ice cores, Antarctica (Etheridge et al., 1996; Monnin et al., 2004). Triangles, this study; squares are samples from the same core measured and discussed by Huang et al. (1999). $\delta^{13}C_{wax}$ values have been corrected for the Suess effect (Verburg, 2007). Bar represents the pooled standard deviation of triplicate samples. (For interpretation of the references to color in this figure, the reader is referred to the web version of this article.)

of Sacred Lake, leading to higher carbon isotopic fractionation in C_3 plants; however, this effect was likely minor (Terashima et al., 1995). We therefore interpret decreasing post-industrial $\delta^{13}C_{wax}$ at Sacred Lake to reflect increasing dominance of C_3 vegetation under increasing atmospheric CO_2 concentrations. Increased CO_2 could also have directly increased the density and biomass of woody C_3 plants in the savannas around Mt. Kenya via direct growth stimulation, as has been found in field experiments on South African savannas (Buitenwerf et al., 2011). Impacts of increased aridity on lowland semi-tropical forests may have exacerbated these effects. Rising temperatures may also have played a role; however, increased temperature favors C_4 plants, and so temperature effects would likely act in opposition to the CO_2 effect unless temperature's role were more indirect (Ehleringer et al., 1997). Similarly, falling lake levels at Sacred Lake should also have favored an increase, not a decrease, in C_4 grasses and sedges in the immediate catchment. Rather, we argue that the relatively cool temperatures at Sacred Lake and elsewhere on Mt. Kenya made these ecosystems particularly sensitive to the post-industrial rise in atmospheric CO_2.

4. Conclusions

Our analysis of leaf waxes at Sacred Lake reveals that Mt. Kenya's climate was highly variable over the past 1800 years. These variations were primarily driven by changes in the amount of Indian Ocean moisture penetrating into East Africa. Early Common Era D-enrichments in δD_{wax} centered around 200C.E. and 690C.E. provide evidence that a weakened Indian Ocean monsoon influenced droughts on a regional scale, while a D-enrichment centered on 1100C.E. was more limited in duration than in other records, suggesting that a weakened Atlantic monsoon played a larger role during this interval, as has been suggested from West African records. Mt. Kenya experienced pronounced hydrologic variability during the Little Ice Age (LIA), with a dry interval from 1450–1700C.E. followed by pluvial conditions until 1850C.E., when a modern drying trend was initiated. Some of these precipitation anomalies may have been highly seasonal in character, with additional effects related to a southward migration of the ITCZ. These mechanisms may help to explain both the spatiotemporal heterogeneity across East African paleoclimate records during this time period, as well as the similarities between our site on Mt. Kenya and Lake Edward in western Uganda/Congo. The vegetation around Sacred Lake responded strongly to post-LIA climate change, with an expansion of C_3 relative to C_4 vegetation that may be tied to a combination of increasing CO_2 and aridity.

Sacred Lake's level is dramatically low today. Our analysis suggests that this pattern of aridification may have begun prior to the 20th century, and could be related to rising temperatures, potentially via lake evaporation and/or reduced cloudiness due to dry conditions.

These findings indicate that the mid-slope region of Mt. Kenya around Sacred Lake is highly sensitive to regional climate variations as well as local feedbacks that are specific to montane regions. Further work is needed to characterize these effects of temperature and greenhouse gases on other tropical montane ecosystems, and to assess potential impacts under 21st century climate change scenarios.

Acknowledgments

This project was supported by the NOAA grant NOAA-NA090AR4310107 to J. Russell, the NOAA grant NA09OAR4310090 and the NSF AGS grant 1003690 to M. Vuille, and by an NSF Graduate Research Fellowship to B. Konecky. We thank two anonymous reviewers for the helpful feedback in improving this manuscript.

Appendix A. Supplementary data

Supplementary data to this article can be found online at http://dx.doi.org/10.1016/j.palaeo.2013.12.037.

References

Alin, S.R., Cohen, A.S., 2003. Lake-level history of Lake Tanganyika, East Africa, for the past 2500 years based on ostracode-inferred water-depth reconstruction. Palaeogeogr. Palaeoclimatol. Palaeoecol. 199, 31–49.
Anchukaitis, K.J., Tierney, J.E., 2012. Identifying coherent spatiotemporal modes in time-uncertain proxy paleoclimate records. Clim. Dyn. http://dx.doi.org/10.1007/s00382-012-1483-0.
Barker, P.A., Street-Perrott, F.A., Leng, M.J., Greenwood, P.B., Swain, D.L., Perrott, R.A., Telford, R.J., Ficken, K.J., 2001. A 14,000-year oxygen isotope record from diatom silica in two alpine lakes on Mt. Kenya. Science 292, 2307–2310.
Bergonzini, L., Richard, Y., Petit, L., Camberlin, P., 2004. Zonal circulations over the Indian and Pacific Oceans and the level of lakes Victoria and Tanganyika. Int. J. Climatol. 24, 1613–1624.
Berke, M.A., Johnson, T.C., Werne, J.P., Grice, K., Schouten, S., Sinninghe Damsté, J.S., 2012a. Molecular records of climate variability and vegetation response since the Late Pleistocene in the Lake Victoria basin, East Africa. Quat. Sci. Rev. 55, 59–74.
Berke, M.A., Johnson, T.C., Werne, J.P., Schouten, S., Sinninghe Damsté, J.S., 2012b. A mid-Holocene thermal maximum at the end of the African Humid Period. Earth Planet. Sci. Lett. 351–352, 95–104.
Bonnefille, R., Mohammed, U., 1994. Pollen-inferred climatic fluctuations in Ethiopia during the last 3000 years. Palaeogeogr. Palaeoclimatol. Palaeoecol. 109, 331–343.
Bradley, R.S., Keimig, F.T., Diaz, H.F., Hardy, D.R., 2009. Recent changes in freezing level heights in the Tropics with implications for the deglacierization of high mountain regions. Geophys. Res. Lett. 36.
Brown, E.T., Johnson, T.C., 2005. Coherence between tropical East African and South American records of the Little Ice Age. Geochem. Geophys. Geosyst. 6, Q12005.
Bruijnzeel, L.A., Mulligan, M., Scatena, F.N., 2011. Hydrometeorology of tropical montane cloud forests: emerging patterns. Hydrol. Process. 25, 465–498.
Buitenwerf, R., Bond, W.J., Stevens, N., Trollope, W.S.W., 2011. Increased tree densities in South African savannas: >50 years of data suggests CO2 as a driver. Global Change Biol. 18, 675–684.
Cockerton, H.E., Street-Perrott, F.A., Leng, M.J., Barker, P.A., Horstwood, M.S.A., Pashley, V., 2013. Stable-isotope (H, O, and Si) evidence for seasonal variations in hydrology and Si cycling from modern waters in the Nile Basin: implications for interpreting the Quaternary record. Quat. Sci. Rev. 66, 4–21.
Coetzee, J., 1964. Evidence for a considerable depression of the vegetation belts during the upper Pleistocene on the East African mountains. Nature 204, 564–566.
Coetzee, J., 1967. Pollen analytical studies in East and Southern Africa. Palaeoecology of Africa and of the surrounding islands and. Palaeoecology of Africa and of the Surrounding Islands and Antarctica, Cape Town/Amsterdam.
Collatz, G.J., Berry, J.A., Clark, J.S., 1998. Effects of climate and atmospheric CO_2 partial pressure on the global distribution of C_4 grasses: present, past, and future. Oecologia 114, 441–454.
Collister, J.W., Rieley, G., Stern, B., Eglinton, G., Fry, B., 1994. Compound-specific $\delta^{13}C$ analyses of leaf lipids from plants with differing carbon dioxide metabolisms. Org. Geochem. 21, 619–627.
Craig, H., Gordon, L.I., 1965. Deuterium and oxygen 18 variations in the ocean and the marine atmosphere. In: Tongiorgi, E. (Ed.), Stable Isotopes in Oceanographic Studies and Paleotemperatures (Spoleto, Italy).
Dagg, M., Blackie, J.R., 1970. Estimates of evaporation in East Africa in relation to climatological classification. Geogr. J. 136, 227–234.
Dansgaard, W., 1964. Stable isotopes in precipitation. Tellus 16, 436–468.
Diefendorf, A.F., Mueller, K.E., Wing, S.L., Koch, P.L., Freeman, K.H., 2010. Global patterns in leaf ^{13}C discrimination and implications for studies of past and future climate. Proc. Natl. Acad. Sci. 107, 5738–5743.
Draxler, R., 1999. HYSPLIT4 User's Guide. NOAA Technical Memorandum ERL ARL-230.
Duane, W.J., Pepin, N.C., Losleben, M.L., Hardy, D.R., 2008. General characteristics of temperature and humidity variability on Kilimanjaro, Tanzania. Arct. Antarct. Alp. Res. 40, 323–334.
Eggermont, H., Heiri, O., Russell, J., Vuille, M., Audenaert, L., Verschuren, D., 2010. Paleotemperature reconstruction in tropical Africa using fossil *Chironomidae* (Insecta: Diptera). J. Paleolimnol. 43, 413–435.
Ehleringer, J.R., Cerling, T.E., Helliker, B.R., 1997. C4 photosynthesis, atmospheric CO2, and climate. Oecologia 112, 285–299.
Etheridge, D.M., Steele, L.P., Langenfelds, R.L., Francey, R.J., Barnola, J.-M., Morgan, V.I., 1996. Natural and anthropogenic changes in atmospheric CO_2 over the last 1000 years from air in Antarctic ice and firn. J. Geophys. Res. 101, 4115.
Ficken, K., Li, B., Swain, D., Eglinton, G., 2000. An n-alkane proxy for the sedimentary input of submerged/floating freshwater aquatic macrophytes. Org. Geochem. 31, 745–749.
Giannini, A., Biasutti, M., Held, I.M., Sobel, A.H., 2008. A global perspective on African climate. Clim. Chang. 90, 359–383.
Goddard, L., Graham, N., 1999. Importance of the Indian Ocean for simulating rainfall anomalies over eastern and southern Africa. J. Geophys. Res.-Atmos. 104, 19099–19116.
Good, S.P., Caylor, K.K., 2011. Climatological determinants of woody cover in Africa. Proc. Natl. Acad. Sci. 108, 4902–4907.
Hastenrath, S., 1984. The Glaciers of Equatorial East Africa. D. Reidel Publishing Company, Dordrecht, Holland.
Hastenrath, S., 2001. Variations of East African climate during the past two centuries. Clim. Chang. 50, 209–217.
Haug, G., Hughen, K., Sigman, D., Peterson, L., Rohl, U., 2001. Southward migration of the intertropical convergence zone through the Holocene. Science 293, 1304–1308.
Heegaard, E., Birks, H., Telford, R., 2005. Relationships between calibrated ages and depth in stratigraphical sequences: an estimation procedure by mixed-effect regression. The Holocene 15, 612–618.

Hemp, A., 2006. Continuum or zonation? Altitudinal gradients in the forest vegetation of Mt. Kilimanjaro. Plant Ecol. 184, 27–42.
Huang, Y., Street-Perrott, F.A., Perrott, R.A., Metzger, P., Eglinton, G., 1999. Glacial–interglacial environmental changes inferred from molecular and compound-specific $\delta^{13}C$ analyses of sediments from Sacred Lake, Mt. Kenya. Geochim. Cosmochim. Acta 63, 1383–1404.
Jolly, D., Haxeltine, A., 1997. Effect of low glacial atmospheric CO2 on tropical African montane vegetation. Science 276, 786–788.
Kebede, S., Travi, Y., 2012. Origin of the $\delta^{18}O$ and $\delta^{2}H$ composition of meteoric waters in Ethiopia. Quat. Int. 257, 4–12.
Konecky, B.L., Russell, J.M., Johnson, T.C., Brown, E.T., Berke, M.A., Werne, J.P., Huang, Y., 2011. Atmospheric circulation patterns during late Pleistocene climate changes at Lake Malawi, Africa. Earth Planet. Sci. Lett. 312, 318–326.
LeGrande, A.N., Schmidt, G.A., 2009. Sources of Holocene variability of oxygen isotopes in paleoclimate archives. Clim. Past 5, 441–455.
Levin, N.E., Zipser, E.J., Cerling, T.E., 2009. Isotopic composition of waters from Ethiopia and Kenya: insights into moisture sources for eastern Africa. J. Geophys. Res. 114, D23306.
Loomis, S.E., Russell, J.M., Ladd, B., Street-Perrott, F.A., Sinninghe Damsté, J.S., 2012. Calibration and application of the branched GDGT temperature proxy on East African lake sediments. Earth Planet. Sci. Lett. 357–358, 277–288.
Majoube, M., 1971. Fractionment en oxygene-18 et en deuterium entré l'eau at sa vapeur. J. Chim. Phys. 1423–1436.
Moelg, T., Cullen, N.J., Hardy, D.R., Winkler, M., Kaser, G., 2009. Quantifying climate change in the tropical midtroposphere over East Africa from glacier shrinkage on Kilimanjaro. J. Clim. 22, 4162–4181.
Monnin, E., Steig, E.J., Siegenthaler, U., Kawamura, K., Schwander, J., Stauffer, B., Stocker, T.F., Morse, D.L., Barnola, J.-M., Bellier, B., 2004. Evidence for substantial accumulation rate variability in Antarctica during the Holocene, through synchronization of CO_2 in the Taylor Dome, Dome C and DML ice cores. Earth and Planetary Science Letters 224, 45–54.
Nicholson, S.E., 1996. A review of climate dynamics and climate variability in eastern Africa. The Limnology, Climatology and Paleoclimatology of the East African Lakes. 25–56.
Nicholson, S., 1997. An analysis of the ENSO signal in the tropical Atlantic and western Indian oceans. Int. J. Climatol. 17, 345–375.
Nicholson, S., 2001. Climatic and environmental change in Africa during the last two centuries. Clim. Res. 17, 123–144.
Nicholson, S., Kim, J., 1997. The relationship of the El Nino–Southern oscillation to African rainfall. Int. J. Climatol. 17, 117–135.
Olago, D.O., Street-Perrott, F.A., Perrott, R.A., Ivanovich, M., Harkness, D.D., 2000. Late Quaternary primary tephras in Sacred Lake sediments, northeast Mount Kenya, Kenya. J. Afr. Earth Sci. 30, 957–969.
O'Leary, M.H., 1981. Carbon isotope fractionation in plants. Phytochemistry 20, 553–567.
Oppo, D.W., Rosenthal, Y., Linsley, B.K., 2009. 2,000-year-long temperature and hydrology reconstructions from the Indo-Pacific warm pool. Nature 460, 1113–1116.
Powers, L.A., Johnson, T.C., Werne, J.P., Castañeda, I.S., Hopmans, E.C., Sinninghe Damsté, J.S., Schouten, S., 2011. Organic geochemical records of environmental variability in Lake Malawi during the last 700 years, Part I: the TEX 86 temperature record. Palaeogeogr. Palaeoclimatol. Palaeoecol. 303, 133–139.
Riley, W.J., Still, C.J., Torn, M.S., Berry, J.A., 2002. A mechanistic model of $H_2^{18}O$ and $C^{18}OO$ fluxes between ecosystems and the atmosphere: model description and sensitivity analyses. Global Biogeochem. Cycles 16, 42-1–42-14.
Russell, J., Johnson, T., 2005. A high-resolution geochemical record from Lake Edward, Uganda Congo and the timing and causes of tropical African drought during the late Holocene. Quat. Sci. Rev. 24, 1375–1389.
Russell, J., Johnson, T., 2007. Little Ice Age drought in equatorial Africa: intertropical convergence zone migrations and El Niño–Southern Oscillation variability. Geology 35, 21.
Sachse, D., Billault, I., Bowen, G.J., Chikaraishi, Y., Dawson, T.E., Feakins, S.J., Freeman, K.H., Magill, C.R., McInerney, F.A., van der Meer, M.T.J., 2012. Molecular paleohydrology: interpreting the hydrogen-isotopic composition of lipid biomarkers from photosynthesizing organisms. Annu. Rev. Earth Planet. Sci. 40, 221–249.
Sage, R.F., 2002. How terrestrial organisms sense, signal, and respond to carbon dioxide. Integr. Comp. Biol. 42, 469–480.
Sage, R.F., Way, D.A., Kubien, D.S., 2008. Rubisco, rubisco activase, and global climate change. J. Exp. Bot. 59, 1581–1595.
Saji, N., Goswami, B., Vinayachandran, P., Yamagata, T., 1999. A dipole mode in the tropical Indian Ocean. Nature 401, 360–363.
Shanahan, T.M., Overpeck, J.T., Anchukaitis, K.J., Beck, J.W., Cole, J.E., Dettman, D.L., Peck, J.A., Scholz, C.A., King, J.W., 2009. Atlantic forcing of persistent drought in West Africa. Science 324, 377–380.
Street-Perrott, F.A., Huang, Y., Perrott, R.A., Eglinton, G., Barker, P., Khelifa, L.B., Harkness, D.D., Olago, D.O., 1997. Impact of lower atmospheric carbon dioxide on tropical mountain ecosystems. Science 278, 1422–1426.
Street-Perrott, F.A., Ficken, K.J., Huang, Y., Eglinton, G., 2004. Late Quaternary changes in carbon cycling on Mt. Kenya, East Africa: an overview of the $\delta^{13}C$ record in lacustrine organic matter. Quat. Sci. Rev. 23, 861–879.
Terashima, I., Masuzawa, T., Ohba, H., Yokoi, Y., 1995. Is photosynthesis suppressed at higher elevations due to low CO_2 pressure? Ecology 76, 2663–2668.
Thompson, B.W., 1966. The mean annual rainfall of Mount Kenya. Weather 21, 48–49.
Thompson, L., Mosley-Thompson, E., Davis, M., Henderson, K., Brecher, H., Zagorodnov, V., Mashiotta, T., Lin, P., Mikhalenko, V., Hardy, D., Beer, J., 2002. Kilimanjaro ice core records: evidence of Holocene climate change in tropical Africa. Science 298, 589–593.
Tierney, J.E., Mayes, M.T., Meyer, N., Johnson, C., Swarzenski, P.W., Cohen, A.S., Russell, J.M., 2010. Late-twentieth-century warming in Lake Tanganyika unprecedented since AD 500. Nat. Geosci. 3, 422–425.
Tierney, J., Russell, J., Sinninghe Damsté, J.S., Huang, Y., Verschuren, D., 2011. Late Quaternary behavior of the East African monsoon and the importance of the Congo Air Boundary. Quat. Sci. Rev. 30, 798–807.
Tierney, J.E., Smerdon, J.E., Anchukaitis, K.J., Seager, R., 2013. Multidecadal variability in East African hydroclimate controlled by the Indian Ocean. Nature 493, 389–392.
Ummenhofer, C.C., Sen Gupta, A., England, M.H., Reason, C.J.C., 2009. Contributions of Indian Ocean sea surface temperatures to enhanced East African rainfall. J. Clim. 22, 993–1013.
Verburg, P., 2007. The need to correct for the Suess effect in the application of $\delta^{13}C$ in sediment of autotrophic Lake Tanganyika, as a productivity proxy in the Anthropocene. J. Paleolimnol. 37, 591–602.
Verschuren, D., 2001. Reconstructing fluctuations of a shallow East African lake during the past 1800 yrs from sediment stratigraphy in a submerged crater basin. J. Paleolimnol. 25, 297–311.
Verschuren, D., 2004. Decadal and century-scale climate variability in tropical Africa during the past 2000 years. In: Battarbee, R.W., Gasse, F., Stickley, C.E. (Eds.), Past Climate Variability Through Europe and Africa. Kluwer Academic Publishers, Dordrecht, The Netherlands, pp. 139–158.
Verschuren, D., Laird, K., Cumming, B., 2000. Rainfall and drought in equatorial east Africa during the past 1,100 years. Nature 403, 410–414.
Vogts, A., Moossen, H., Rommerskirchen, F., Rullkötter, J., 2009. Distribution patterns and stable carbon isotopic composition of alkanes and alkan-1-ols from plant waxes of African rain forest and savanna C3 species. Org. Geochem. 40, 1037–1054.
Vuille, M., Werner, M., Bradley, R.S., Chan, R.Y., Keimig, F., 2005. Stable isotopes in East African precipitation record Indian Ocean zonal mode. Geophys. Res. Lett. 32 (21), L21705.
Wooller, M.J., Swain, D.L., Street-Perrott, F.A., Mathai, S., Agnew, A., 2001. An altitudinal and stable carbon isotope survey of C3 and C4 graminoids on Mount Kenya. J. East Afr. Nat. Hist. 90, 69–85.
Worden, J., Noone, D., Bowman, K., Beer, R., Eldering, A., Fisher, B., Gunson, M., Goldman, A., Herman, R., Kulawik, S.S., Lampel, M., Osterman, G., Rinsland, C., Rodgers, C., Sander, S., Shephard, M., Webster, C.R., Worden, H., 2007. Importance of rain evaporation and continental convection in the tropical water cycle. Nature 445, 528–532.
Zhang, P., Cheng, H., Edwards, R.L., Chen, F., Wang, Y., Yang, X., Liu, J., Tan, M., Wang, X., Liu, J., An, C., Dai, Z., Zhou, J., Zhang, D., Jia, J., Jin, L., Johnson, K.R., 2008. A test of climate, sun, and culture relationships from an 1810-year Chinese cave record. Science 322, 940–942.